Temperature and magnetism bi-responsive molecularly imprinted polymers: preparation, adsorption mechanism and properties as drug delivery system for sustained release of 5-fluorouracil

Longfei Li[ab], Lin Chen[ab], Huan Zhang[ac], Yongzhen Yang[ab,1], Xuguang Liu[ac,1] and Yongkang Chen[ad]

a. Key Laboratory of Interface Science and Engineering in Advanced Materials (Taiyuan University of Technology), Ministry of Education, Taiyuan 030024, China;
b. Research Center on Advanced Materials Science and Technology, Taiyuan University of Technology, Taiyuan 030024, China;
c. College of Chemistry and Chemical Engineering, Taiyuan University of Technology, Taiyuan 030024, China;
d. University of Hertfordshire, School of Engineering and Technology, Hatfield, Hertfordshire AL10 9AB, UK.

Abstract:

Temperature and magnetism bi-responsive molecularly imprinted polymers (TMMIPs) based on Fe_3O_4-encapsulating carbon nanospheres were prepared by free radical polymerization, and applied to selective adsorption and controlled release of 5-fluorouracil (5-FU) from aqueous solution. Characterization results show that the as-synthesized TMMIPs have an average diameter of about 150 nm with a typical core-shell structure, and the thickness of the coating layer is approximately 50 nm. TMMIPs also displayed obvious magnetic properties and thermo-sensitivity. The adsorption results show that the prepared TMMIPs exhibit good adsorption capacity (up to 96.53 mg/g at 25℃) and recognition towards 5-FU. The studies on 5-FU loading and release in vitro suggest that the release rate increases with increasing temperature. Meanwhile, adsorption mechanism were explored by using a computational analysis to simulate the imprinted site towards 5-FU. The interaction energy between imprinted site and 5-FU is -112.24 kJ/mol, originating from hydrogen bond, Van der Waals forces and hydrophobic interaction between functional groups located on 5-FU and NIPAM monomer. The electrostatic potential charges and population analysis results suggest that imprinted site of 5-FU can be introduced on the surface of TMMIPs, confirming their selective adsorption behavior for 5-FU.

Keywords: molecular imprinting technique; temperature-sensitivity; magnetism; drug delivery system; simulate; imprinted site

1. Introduction

5-Fluorouracil (5-FU) is an anticancer drug widely used in the clinical treatment of several solid cancers such as breast, liver and brain cancer. Generally, the

[1]Corresponding author at: Taiyuan University of Technology, 79, West Yingze Street, Taiyuan 030024, China.
Tel/Fax: +86-0351-6014138.
E-mail address: yyztyut@126.com; liuxuguang@tyut.edu.cn.

42 maintenance of serum concentrations of drugs can exert the effect of pharmacological

43 activity. However, 5-FU is soon metabolized in the body, and its half-life is less than

44 20 min [1]. Nowadays, a particular issue for most anticancer drugs is the effect

45 feedback-controlled release, and the maintenance of a therapeutic level of a drug

46 within both the drug reservoir and the target site [2]. This requires a drug delivery

47 system with molecular recognition properties, such that it is able to bind and release

48 only very specific molecular species. Therefore, molecularly imprinted polymers

49 (MIPs) have been researched as the drug delivery system owing to their molecular

50 recognition properties [3-7].

51 Molecular imprinting technique is an emerging technique, which is a powerful

52 synthesis method for creation of specific binding sites in MIPs. Owing to the highly

53 selective recognition, and excellent adsorption to the template and its analogue, the

54 promising applications for these MIPs include molecular recognition materials for

55 biosensors, simulated enzyme catalysis, antibody mimics, selective solid adsorbents,

56 drug delivery system and so on [8-12]. Recently, the smart molecular imprinting

57 technology has aroused great interests in the field of biomedicine. The temperature

58 and magnetism bi-responsive molecularly imprinted polymers (TMMIPs), as a new

59 class of smart MIPs, show great superiority over the others, especially as drug

60 delivery system. In drug delivery system, TMMIPs have many advantages, such as

61 superparamagnetism, high selectivity and temperature-sensitivity. Under the external

62 magnetic field, they can be applied to the orientation, positioning and controllable

63 separation, as well as the controlled release through the temperature-sensitive polymer

64 which responses to the magnetocaloric effect [13].

65 Temperature-sensitive polymer is sensitive to temperature because of its smart

66 structure，such as poly(2-(dimethylamino) ethyl methacrylate) [14], poly(methacrylic

67 acid) [15] and poly (N-isopropylacrylamide) (PNIPAM) [16]. Among them PNIPAM

68 has a lower critical solution temperature (LCST) and reversible solubility in an

69 aqueous solution around $32\,℃$, which is close to physiological temperature.

70 Consequently, when temperature is below the LCST temperature, it can be fully

71 soluble and form a homogeneous system. However, as the temperature is increased

72 above the LCST, it switches from hydrophilic state to hydrophobic state, and

73 precipitates from the aqueous solution. When temperature-sensitive polymer is

74 integrated with MIPs, the ability of the resulting imprinted polymer in capturing and

75 releasing template molecules can be adjusted by external temperature [16-21].

76 Nowadays, the temperature-sensitive imprinted polymers (TMIPs) as an important

77 part of smart drug delivery system have been reported. Pan et al [22] prepared TMIPs

78 by using antibiotic drug cephalexin as template molecule and N-isopropylacrylamide

79 (NIPAM) as the temperature-responsive monomer. Results indicated that TMIPs have

80 a good ability to identify molecule with excellent temperature response capability.

81 Moreover, targeted drug delivery is also a significant property in drug delivery system.

82 As we all know, Fe_3O_4 magnetic nanoparticles are a common magnetic-targeting

83 materials because of their excellent properties, such as superparamagnetism,

84 biocompatibility, low toxicity and easy modification with different functional groups

according to need [23, 24]. Currently, a few recently conducted researches about TMMIPs have been reported. Xu et al [25] prepared TMMIPs to remove antibiotics from aqueous solution. Similarly, You et al [26] prepared high-capacity TMMIPs for selective extraction of curcuminoids. From above-mentioned research results, it can be seen that TMMIPs have good temperature response, superparamagnetism and recognition ability. In view of their prominent properties, TMMIPs may be applied in controlled drug release to match actual physiological needs at a proper site and time [27]. Nevertheless, so far, there are few reports about the use of TMMIPs as drug delivery system.

Here, TMMIPs were prepared by surface grafting copolymerization method. The synthesis route and thermosensitivity of TMMIPs is shown in Fig.1. Firstly, Fe_3O_4-encapsulating carbon ($Fe_3O_4@C$) nanospheres were prepared by solvothermal method, and the silanization of $Fe_3O_4@C$ nanospheres ($Fe_3O_4@C_{Si}$) with activated surface was realized by the modification of 3-(trimethoxysilyl)propyl methacrylate (MPS). Secondly, NIPAM was chosen as the temperature-sensitive functional monomer and grafted on the surface of $Fe_3O_4@C_{Si}$ nanospheres (the products are named as $Fe_3O_4@C_{Si}@PNIPAM$). Finally, TMMIPs were prepared by using $Fe_3O_4@C_{Si}@PNIPAM$ as matrix material, 5-FU as template, and N, N'-methylene bisacrylamide (MBA) as cross linker. Subsequently, TMMIPs were systematically characterized by field emission scanning electron microscopy (FESEM), transmission electron microscopy (TEM), Fourier transformation infrared spectroscopy (FT-IR), thermogravimetry (TG), UV-Visible spectrophotometer (UV-Vis), dynamic light scattering (DLS) and vibrating sample magnetometry (VSM). The adsorption capacity and controllable release of 5-FU were investigated through adsorption kinetics, adsorption isotherms, selective adsorption and release experiments. The interaction between 5-FU and NIPAM was also investigated by using Materials Studio DMol^3 program. The theoretical model of the imprinted site towards 5-FU was proposed and used for evaluation of the TMMIPs affinity towards 5-FU [28-32].
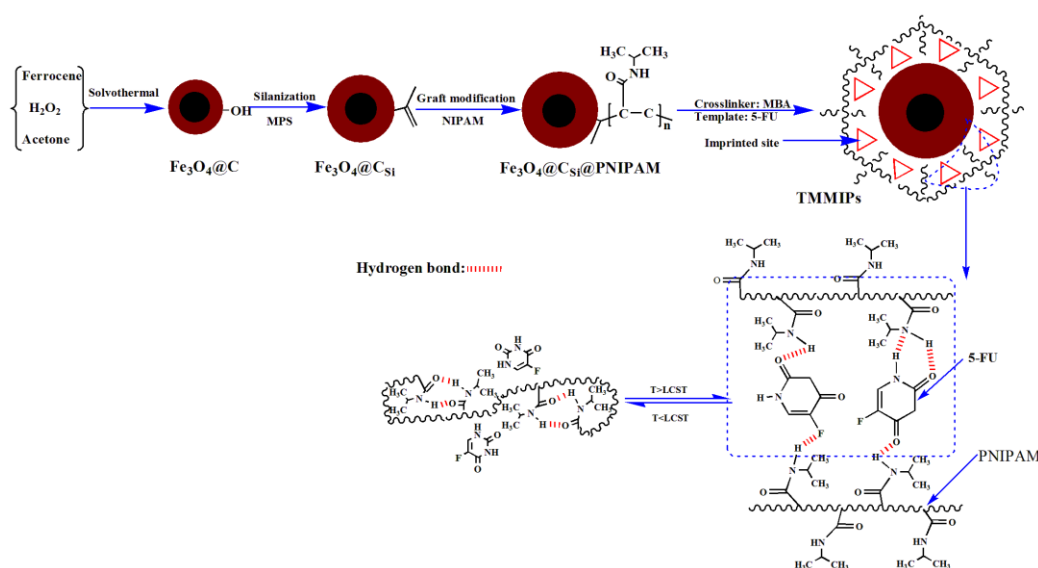
Fig. 1. Synthesis routes of TMMIPs and the reversible thermosensitive swelling/ shrinking transition of TMMIPs.

2. Experimental

2.1 Materials

NIPAM, 5-FU, MBA and phosphate buffered saline (PBS) were purchased from Aladdin. Ferroncene, hydrogen peroxide (30% H_2O_2, wt), ammonium persulfate (APS), acetic acid and MPS were purchased from Tianjin Dongli Chemical Reagent Factory, China. Deionized water was used in all experiments.

2.2 Preparation of $Fe_3O_4@C_{Si}$ nanospheres

$Fe_3O_4@C_{Si}$ nanospheres with magnetic properties were synthesized via a reported two-step process [33]. Firstly, 1.2 g of ferrocene iron was dissolved in 40 mL of acetone, followed by addition of 2.0 mL of H_2O_2. The mixture solution was sonicated for 10 min and then sealed in 50 mL teflon-lined stainless-steel autoclave, maintained at 180℃ for 48 h. Subsequently, the products were collected with the help of an external magnetic field, washed with ethanol and deionized water several times, and dried in a vacuum oven at 50℃ to give $Fe_3O_4@C$ nanospheres. Secondly, MPS was used as the coupling agent to introduce C=C onto the surface of the $Fe_3O_4@C$ nanospheres. Briefly, 0.2 g of $Fe_3O_4@C$ nanospheres was dispersed in 60 mL of mixture solvent of ethanol and deionized water (v:v = 2:1) followed by addition of MPS (2 mL) and adjustment of pH to 5.0 by acetic acid. Then the mixture solution was sonicated for 10 min, and transferred to a thermostat water bath with mechanical stirring at 65℃. The mixture was refluxed under N_2 atmosphere for 4 h. Finally, the products were washed with ethanol, and collected with the help of an external magnetic field, and dried overnight under vacuum to get $Fe_3O_4@C_{Si}$ nanospheres.

2.3 Synthesis of $Fe_3O_4@C_{Si}@PNIPAM$ nanospheres

Here, thermo-sensitive property was introduced by grafting NIPAM monomer on the surface of $Fe_3O_4@C_{Si}$ nanospheres. The preparation process of $Fe_3O_4@C_{Si}@PNIPAM$ nanospheres is as follows: 0.2 g of $Fe_3O_4@C_{Si}$ nanospheres was added to 30.0 mL of deionized water and sonicated for 10 min. Subsequently, 0.04 g of APS was added to induce free radical from the surface of $Fe_3O_4@C_{Si}$. Then, 0.4 g of NIPAM monomer was added. All the processes were carried out under N_2 atmosphere. The reaction was initiated at 70℃ and lasted for 10 h under mild stirring. The products were collected by an external magnetic field, then dried overnight under vacuum, and named as $Fe_3O_4@C_{Si}@PNIPAM$.

2.4. Preparation of TMMIPs

TMMIPs were synthesized by using 5-FU as template, APS as initiator, and MBA as cross-linking agent. Briefly, 0.2 g of $Fe_3O_4@C_{Si}@PNIPAM$ nanospheres was dissolved into 30 mL of PBS (pH=7.4). When the temperature rose to 65℃ under N_2 atmosphere, 5 mg of APS was added to induce free radical from the surface of $Fe_3O_4@C_{Si}@PNIPAM$. Subsequently, 40 mg of MBA and 0.1 g of 5-FU was

successively added for cross-linking over 10 h. Finally the products were washed by methanol and water (v/v, 4:1) several times, and collected with the help of an external magnetic field, and dried overnight under vacuum to get TMMIPs. For comparison, the preparation of temperature-sensitive magnetic molecularly non-imprinted nanospheres (TMNIPs) was carried out with the same procedure as that of TMMIPs, just without 5-FU as template molecule.

2.5 Adsorption experiment

For equilibrium experiments, 5.0 mg of TMMIPs (or TMNIPs) was suspended in 10 mL of a series of 5-FU solutions with initial concentrations ranging from 1 to 5 mmol/L. The series of mixtures were shaken for 400 min at 25℃ and 45℃, separately. Then the equilibrium concentrations of 5-FU were detected by UV-Vis analysis.

The equilibrium adsorption capacity Q_e (mg/g) was calculated according to the equation (1):

$$Q_e = (C_0 - C_e)M \, V/m \tag{1}$$

where C_0 (mmol/L) represents the initial concentration of 5-FU, C_e (mmol/L) is the equilibrium concentration of 5-FU, M (g/mol) is the molar mass of 5-FU, V (L) is the volume of 5-FU solution, while m (g) means the mass of TMMIPs or TMNIPs.

Similarly, for kinetic experiments, 10 mg of TMMIPs (or TMNIPs) was suspended in 25 mL of 5 mmol/L 5-FU solution. Then the mixtures were continuously shaken at 25℃, and the concentration of 5-FU in the supernatant at a certain time intervals (10, 20, 40, 60, 90, 120, 180, 240, 360 and 480 min) was analyzed by UV-Vis, and then the adsorption capacity Q_t (mg/g) at different contact time was calculated as the equation (2):

$$Q_t = (C_0 - C_t)M \, V/m \tag{2}$$

where C_t (mmol/L) is the concentration of 5-FU at different contact time, C_0, M, V and m are the same as for Eq.1.

Selective adsorption was performed by using three kinds of pyrimidine (5-FU, thymine and uracil) in individual standard solution with the same initial concentration (5 mmol/L).

2.6 Release experiment

The release of 5-FU from TMMIPs or TMNIPs was carried out as follows: TMMIPs (or TMNIPs) (20 mg) was immersed in 50 mL of 5 mmol/L 5-FU solution for 24 h at 25℃ to reach adsorption equilibrium. Then, TMMIPs (or TMNIPs) capturing 5-FU were separated under an external magnetic field, washed with deionized water, and dried at 50℃ for 12 h. Whereafter, TMMIPs or TMNIPs were placed into 20 mL of PBS at 25℃, sampled 4 mL solution at regular time intervals, and then supplemented with the same volume of PBS to maintain a constant volume of total solution. 5-FU in the released solution was determined by UV-Vis. The percent release capacity Q (%) was calculated according to the equation (3):

$$Q\left(\%\right)=\frac{\left(C_n \times V_0 + V_i \sum_{i=1}^{n-1} C_i\right)M}{m} \tag{3}$$

Where Q (%) is the cumulative release rate of 5-FU, C_n (mmol/L) is the concentration of 5-FU after the n-th sampling, V_0 (mL) is the total volume of 5-FU solution, V_i (mL) is the sampling volume, C_i (mmol/L) is the concentration of 5-FU at the i-th sampling, while m (g) means the mass of TMMIPs or TMNIPs. The percent release capacity of TMMIPs was also discussed at 25, 35 and 45℃, separately.

2.7 Molecular modeling

In order to research the adsorption mechanism, the simulation was carried out using the ab initio quantum chemistry package, DMol^3 code available from Materials Studio 5.5. Base on the density function theory (DFT), the geometries of all compounds were optimized using the DFT (GGA/PBE) level. All electron calculations were performed with double numerical polarization (DNP) basis set. Self-consistent field procedure was carried out with a convergence criterion of 10^{-5} a.u. for both electrostatics and population analysis. TS method DFT-D correction was used for dispersion corrections. Moreover, considering water solvent effect, the conductor-like screening model (COSMO) implemented into DMol^3 was also used. Here, water was chosen as the solvent, of which permittivity is 78.54 [30, 32, 34, 35].
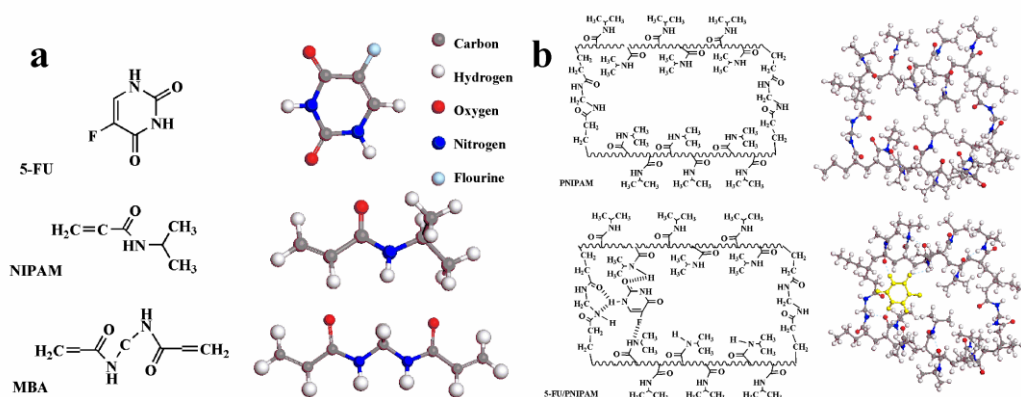

Fig. 2.(a) Chemical formula and conformation of 5-FU, NIPAM and MBA; (b) Chemical formula and conformation of PNIPAM and 5-FU/PNIPAM complex (The yellow molecular in Fig. 2(b) is 5-FU).

With the purpose of studying the interaction between 5-FU and NIPAM, the polymer matrix (PNIPAM) was constructed from the functional monomer (NIPAM) and the cross-linker (MBA). The three-dimensional structure of 5-FU, PNIPAM and multimolecular complex (5-FU/PNIPAM) are shown in Fig. 2.

Interaction energy (ΔE) was calculated from the equation (4) [28]:

$$\Delta E = E_{(5\text{-}FU/PNIPAM)} - [E_{(5\text{-}FU)} + E_{(PNIPAM)}] \tag{4}$$

where E is the total energy of the compound and the complex of compounds. Higher

absolute E value predicts higher binding energy following more stable conformation.

2.8 Characterization and measurements

The morphology and microstructures of the functionalized nanospheres were characterized by FESEM (JSM-6700F, operated at 10 kV, Japan) and TEM (JEOL JEM 2100, electron microscope operating at an acceleration voltage of 60 kV, Japan). Magnetic properties were measured using a vibrating sample magnetometer (VSM, 7300, Lakeshore，USA). TG analysis was carried out on a TG analyzer (Netzsch**,** TG 209 F3, Germany) instrument from 100 to 900℃ in air atmosphere with a heating rate of 10℃/min. The introduction and formation of various functional groups on the surface of Fe_3O_4@C nanospheres were probed by using FT-IR (Bruker Tensor 27, Germany). Average hydrodynamic diameter was measured using DLS at a Zetasizer Nano-ZS90 (Malvern Instruments, UK). The thermosensitivity and adsorption capacity of the TMMIPs (or TMNIPs) were tested using UV-Vis (Shimadzu, UV-3900, Japan).

The interaction between 5-FU and NIPAM in aqueous solution was also investigated by UV-Vis. Briefly, different molar ratios of 5-FU/NIPAM were dissolved in deionized water and scanned from 190 to 400 nm with a speed of 300 nm/min. Meanwhile, deionized water was chosen as background subtraction.

3. Results and discussion

3.1 Structure and magnetic property of TMMIPs

The morphology and microstructure of products were examined by FESEM and TEM. As shown in Fig. 3(a-b), TMMIPs have a uniform, discrete spherical shape with an average diameter of 152 nm (as shown in inset of Fig.3(a)), indicating they are highly monodispersed. The rough surface may be due to the grafted polymer. From the TEM images of TMMIPs in Fig. 3(c, d), a typical core-shell structure is observed in which an amorphous coating layer covers the inner magnetite cores consisting of multiple Fe_3O_4 nanoparticles. As in the previous work [33], the coating layer of Fe_3O_4@C nanospheres has an average thickness of 30 nm. Here, the thickness of coating layer of TMMIPs (in Fig. 3(c, d)) increases to about 50 nm. It is verified that the functional monomer has been grafted on the surface of Fe_3O_4@C nanospheres. However, as the carbon layer and PNIPAM polymer have the same contrast in the dried state, it is difficult to distinguish how thick the polymer layer is.
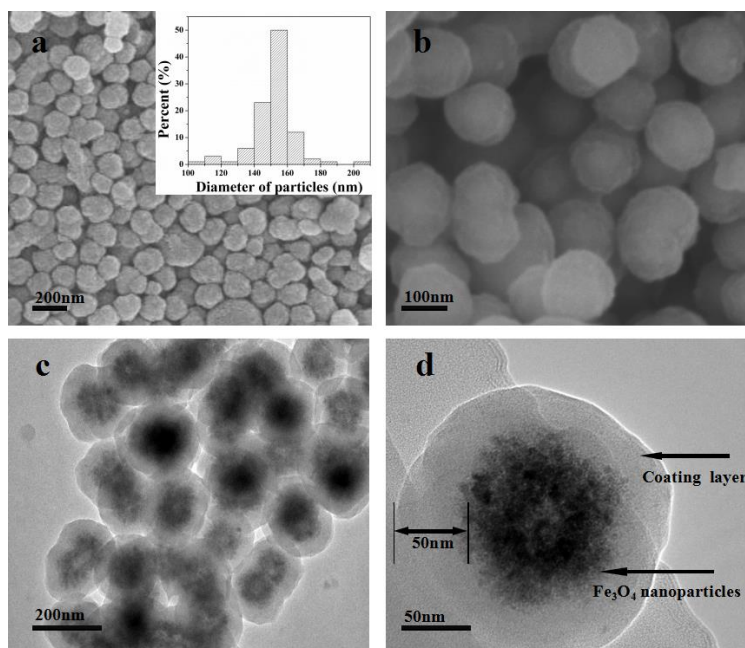
266
267 Fig. 3. FESEM (a, b) and TEM (c, d) images of TMMIPs; size distribution of TMMIPs (inset of (a))
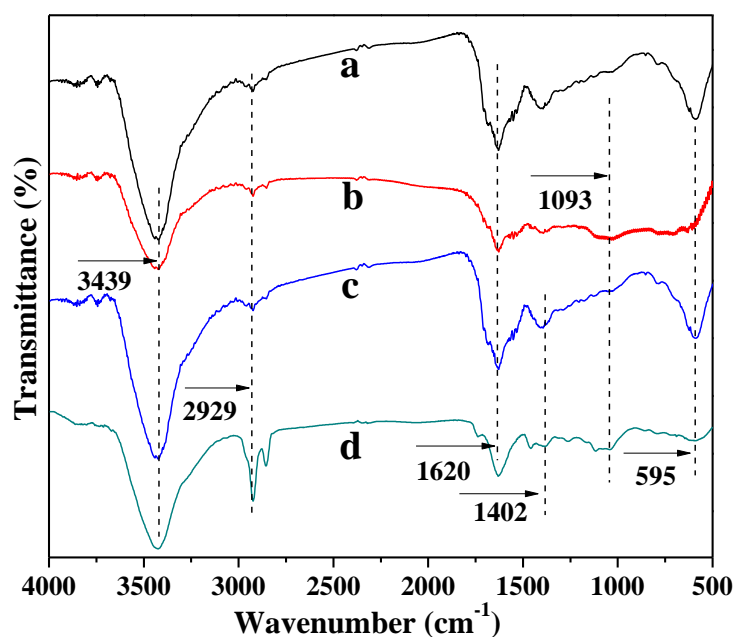268

269
270 Fig. 4. The FT-IR spectra of Fe_3O_4@C (a), Fe_3O_4@C_{Si} (b), Fe_3O_4@C@PNIPAM (c) and TMMIPs (d) nanospheres
271

272   FT-IR measurement was applied to detect the surface functional groups of the
273 Fe_3O_4@C, Fe_3O_4@C_{Si}, Fe_3O_4@C_{Si}@PNIPAM and TMMIPs. In the FT-IR spectra
274 (Fig. 4), the strong bands at 3439 and 1620 cm^{-1} correspond to the –OH and C=O
275 groups, respectively. The Fe–O characteristic band at 595 cm^{-1} is indicative of Fe_3O_4.
276 Compared with Fe_3O_4@C, Fe_3O_4@C_{Si} shows a new band at 1093 cm^{-1}, which can be
277 attributed to Si–O groups. Bands at 2929 cm^{-1} are assigned to the asymmetrical and
278 symmetrical stretching vibration of C–H in MPS. The FT-IR spectra of

8

279     $Fe_3O_4@C_{Si}$ and TMMIPs also clearly show the characteristic bands of
280   –OH, C–H and C=O stretching vibration, and bands at 1402 cm^{-1} (deformation of
281   methyl groups on –CH $(CH_3)_2$) could be attributed to the characteristic bands of
282   PNIPAM [22, 36]. So it can be concluded that NIPAM monomer is grafted on the
283   surface of $Fe_3O_4@C_{Si}$, and the TMMIPs are prepared.

284   TG measurement was applied to further investigate the modification effects of
285     $Fe_3O_4@C_{Si}$. As is seen in Fig. 5, the weight retention of $Fe_3O_4@C_{Si}$ and
286     $Fe_3O_4@C_{Si}@PNIPAM$ is 55.75 % and 49.74 %, respectively. After polymerization,
287   the higher weight loss illustrates the grating of polymer onto the surface of
288     $Fe_3O_4@C_{Si}$. And the remaining weight could be attributed to the stability of Fe_2O_3 and
289   SiO_2. The weight retention at 600℃ obtained for TMMIPs and TMNIPs is 48.68 %
290   and 48.41 %, respectively. The slight weight difference may be attributed to the
291   template molecules, which leads to the different grafting density of polymer in
292   polymerization [37]. So it is believed that thermosensitive polymers are grafted onto
293   the surface of $Fe_3O_4@C_{Si}$ nanospheres and the monomer grafting yield of TMMIPs is
294   about 7.07%.

295
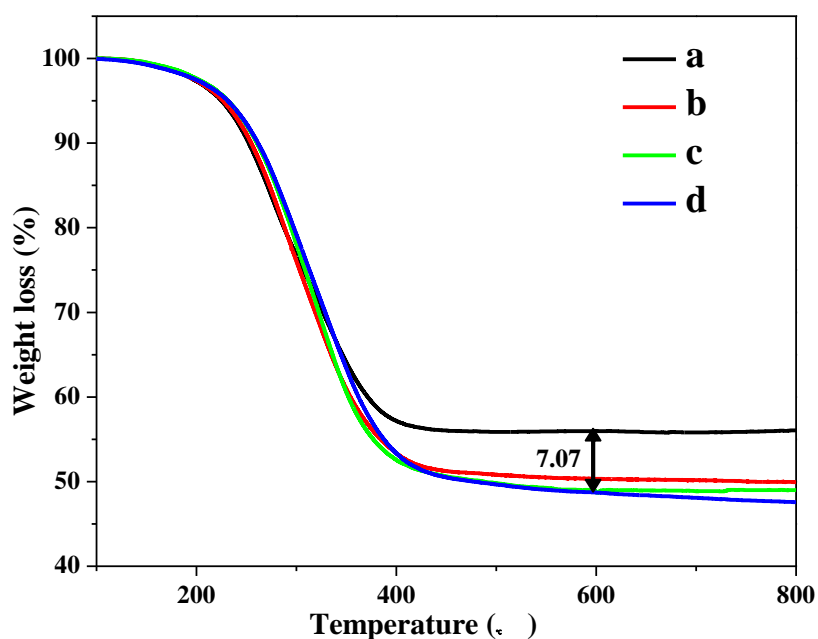
296
297   Fig. 5. TG curves of as-synthesized $Fe_3O_4@C_{Si}$(a), $Fe_3O_4@C_{Si}@PNIPAM$(b), TMMIPs(c) and TMNIPs(d) under
298   air atmosphere (10℃/min).

299
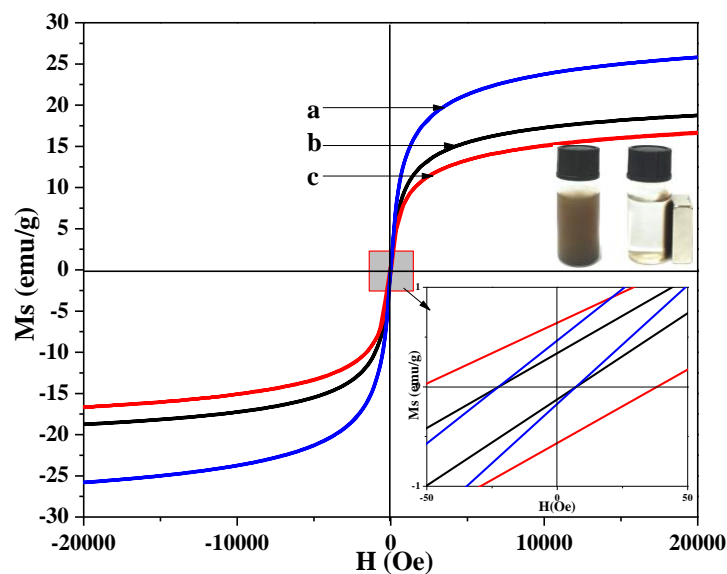
300   Magnetic property is vital to magnetic nanospheres for their applications in drug
301   delivery system. So the magnetic properties of $Fe_3O_4@C$, $Fe_3O_4@C_{Si}@NIPAM$ and
302   TMMIPs were investigated by VSM. Hysteresis loops are shown in Fig. 6. Obviously,
303   there are hardly any magnetic hysteresis, indicating the superparamagnetic nature of
304     $Fe_3O_4@C$, $Fe_3O_4@C@NIPAM$ and TMMIPs. The saturation magnetization of
305     $Fe_3O_4@C$, $Fe_3O_4@C@NIPAM$ and TMMIPs is 25.86, 18.75 and 16.57 emu/g,
306   respectively. It is obviously seen that the saturation magnetization gradually declines
307   after the sample modification as a result of the introduction of non-magnetic moieties.

9

From the picture on the top right corner of Fig.6, these magnetic nanospheres can still be rapidly and completely separated from a suspension by a strong magnet, although the magnetic response of TMMIPs decreases to some content after the formation of the PNIPAM layer [12, 23], which also verify that the functional monomer is grafted on the surface of Fe_3O_4@C.

Magnetic nanoparticles of Fe_3O_4 play two roles during their application in this study. Firstly, they were generally used to target at specific tumors in the presence of an external magnetic field during the application of TMMIPs. Fe_3O_4 nanoparticles could also be used for easy separation or directional move during absorbance and release of 5-FU. Secondly, Fe_3O_4 nanoparticles have a potential to realize magnetic targeting hyperthermia under alternative magnetic field. Such thermal energy could induce the phase transition of temperature-responsive polymer and realize controlled release by magnetism regulation. Drug loading magnetic composite TMMIPs could simultaneously achieve drug targeting, controlled drug release and hyperthermia treatment owing to the superparamagnetic nature, which is greatly significant for practical applications. [38, 39]

Fig. 6. Magnetization curves of Fe_3O_4@C (a), Fe_3O_4@C$_{Si}$@PNIPAM (b) and TMMIPs (c); photograph (inset) of magnetic separation for TMMIPs.

3.2. Temperature-induced phase transition of the TMMIPs

DLS and UV-Vis methods were used to characterize the thermo-sensitive transition of TMMIPs in aqueous solution. The hydrodynamic diameter of TMMIPs as a function of temperature is given in Fig. 7(a). It is found that the hydrodynamic diameter of TMMIPs decreases from 282 to 214 nm as the temperature increases from 20 to 65℃. The results demonstrate that LCST of TMMIPs occurs at around 39.3℃, which is higher than that of pure PNIPAM homopolymer (around 32℃), because of the incorporation of hydrophobic polymer or the restriction of movement of polymer chains imposed by rigid support. As expected, this behavior comes from the shrinkage

10

of PNIPAM shell. When the temperature is below LCST, hydrogen bonds between hydrophilic groups of polymer chains are dominant. These bonds become weaker and hydrophobic interactions between polymer chains become stronger when temperature is elevated over LCST [25]. In addition, as the Fig. 7(b) shows, the absorbance of TMMIPs aqueous solution (400 mg/L) at different temperature has little change from 20 to 30℃. The peak at 402 nm increases from 1 to 1.5 between 30 and 60℃, and the change trend of absorbance was similar to those of water solution of pure PNIPAM. When the temperature is above LCST, PNIPAM shrink to become hydrophobic, and the change trend of absorbance is mainly attributed to the temperature-dependent solubility of PNIPAM in water. [18] The results show that TMMIPs have excellent temperature-responsive property.
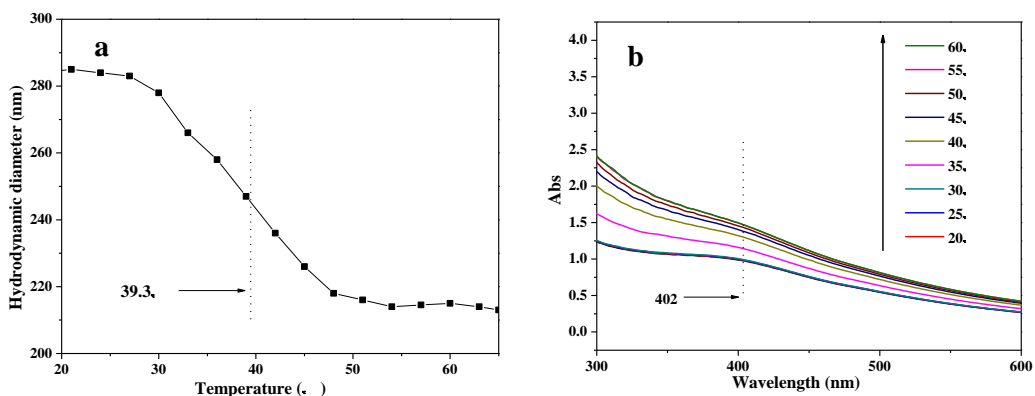
Fig. 7. (a) Hydrodynamic diameters of TMMIPs; (b) UV-Vis absorbance of TMMIPs aqueous solution (400 mg/L) at different temperatures.

3.3 Adsorption isotherm of TMMIPs

The binding parameters of TMMIPs (or TMNIPs) were extracted from the effect of initial 5-FU concentration on adsorption capacity (Fig. 8). The data were obtained by fitting Langmuir and Freundlich adsorption equations as the equation (5) and (6) [40, 41]:

$$Q_e = K_L Q_m C_e / (1 + K_L C_e) \tag{5}$$

$$Q_e = K_F C_e^{1/n} \tag{6}$$

where Q_e (mg/g) is the equilibrium adsorption capacity, C_e (mmol/L) is the equilibrium concentration of 5-FU, Q_m (mg/g) is the maximum adsorption capacity of the sorbent, K_L (L/mmol) is the adsorption constant, K_F and n are the adsorption equilibrium constants. The calculated values are listed in Table 1.

From Fig. 8, it can be observed that the equilibrium adsorption capacity Q_e for 5-FU increases with increasing equilibrium concentration of 5-FU. This can be attributed to the accelerated diffusion of 5-FU molecules onto TMMIPs by the increase in 5-FU concentration. TMMIPs have a higher 5-FU binding capacity than TMNIPs, and the Q_e value of TMMIPs is about 1.5 times that of TMNIPs, suggesting TMMIPs have an excellent binding ability of 5-FU at 25℃. The maximum adsorption capacity of TMMIPs is 96.53 mg/g around 25℃, at this temperature the cavity of TMMIPs is in the imprinted state. As the temperature increases, the shrinking of

11

TMMIPs makes the polymer more hydrophobic, the intermolecular hydrogen band will be formed, and the competitive adsorption between water and 5-FU molecule may also make the Q_e of TMMIPs lower. On the other hand, because there are no specific binding sites in TMNIPs, smaller absorption capacity change is observed for TMNIPs when the temperatures changes.

Langmuir model assumes that the binding sites are homogeneously distributed over the adsorbent surface with monolayer coverage and uniform energies, while Freundlich model is an empirical model based on multilayer adsorption on heterogeneous surfaces with the exponential distribution of active sites and energy [42]. By comparing correlation coefficient (R^2) presented in Table 1, it can be concluded that both the Freundlich and Langmuir model fit the equilibrium data. As shown in Table 1, 1/n of TMMIPs is much smaller than that of TMNIPs, indicating that adsorption is highly favourable for TMMIPs. The Freundlich K_F values follow an order of TMMIPs > TMNIPs, implying that imprinting is an effective method to improve the adsorption capacity and specificity to 5-FU [43].
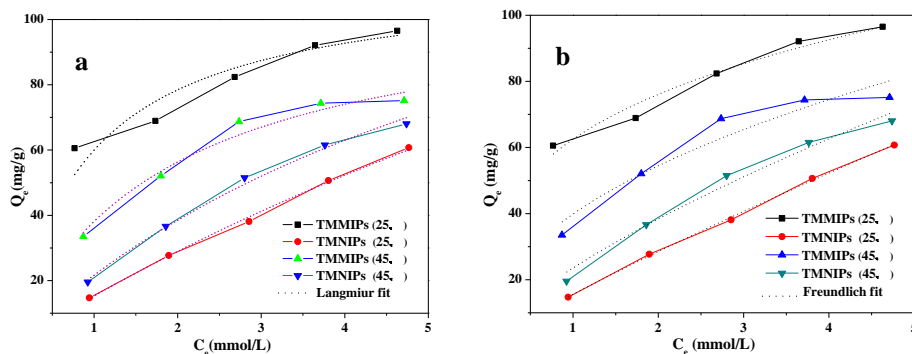
Fig. 8. Adsorption isotherms of 5-FU onto TMMIPs and TMNIPs.

Table 1. Langmuir and Freundlich isotherm constants of TMMIPs and TMNIPs.

| Type of nanospheres	T (℃)	Langmuir			Freundlich		
		Q_m (mg/g)	K_L (L/mmol)	R^2	K_F	1/n	R^2
TMMIPs	25	93.853	1.1238	0.9823	62.4896	0.2835	0.9604
TMNIPs	25	60.803	0.0604	0.9080	16.8821	0.8557	0.9986
TMMIPs	45	77.525	0.5463	0.9762	39.8588	0.4510	0.9144
TMNIPS	45	70.344	0.1432	0.9496	22.9168	0.7471	0.9790

3.4 Adsorption kinetics of TMMIPs

The binding kinetics of TMMIPs (or TMNIPs) at 25℃ are given in Fig. 9. To identify whether the mechanism of 5-FU adsorption depends on the physical or chemical characteristics of the adsorbent, the binding data were analyzed using the pseudo-first-order and pseudo-second-order rate equations [44, 45], separately, which are described by the following equations (7) and (8):

$$\ln(Q_e - Q_t) = \ln Q_e - k_1 t \tag{7}$$

$$t/Q_t = 1/k_2Q_e^2 + t/Q_e \qquad (8)$$

where Q_e (mg/g) and Q_t (mg/g) are the amounts of 5-FU bound on sorbents at equilibrium and at various times t (min), respectively, k_1 (/min) is the rate constant of pseudo-first-order model of adsorption, k_2 (g/(mg·min)) is the rate constant of pseudo-second-order model of adsorption, which can be obtained from the linear fitting of t/Q_t versus t.

The adsorption rate constants and related regression values are summarized in Table 2. The adsorption capacity of 5-FU on TMMIPs (or TMNIPs) increases rapidly at the initial stages, and then gradually flattens. Compared with TMNIPs, TMMIPs reach a higher adsorption capacity. This fact can be attributed to the specific binding sites on the surface of TMMIPs. As shown in Table 2, TMMIPs R^2 value for the pseudo-second-order kinetics exceeds 0.99, much higher than that for the pseudo-first-order models. Furthermore, the calculated adsorption capacity ($Q_{e,cal}$) from the pseudo-second-order kinetics is in accordance with the experimental adsorption capacity, further indicating that 5-FU adsorption over TMMIPs (or TMNIPs) predominantly conforms to the pseudo-second-order kinetics. So it is suggested that the chemical adsorption process could be the mainly rate-limiting step in the adsorption process for 5-FU [44].
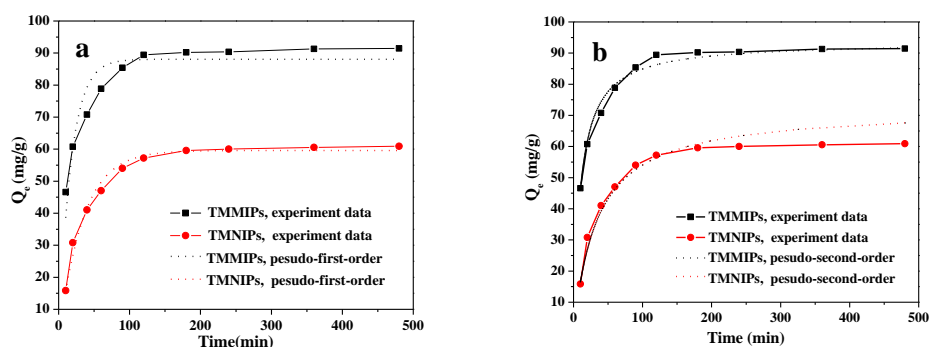
Fig. 9. Effect of contact time on the adsorption of 5-FU (5mmol/L) on TMMIPs and TMNIPs at 25℃. The dotted line is the model simulation and the solid line is experiment data.

Table 2. Kinetic constants for pseudo-first-order equation and pseudo-second order equation at 25℃.

Adsorption kinetics models	Constants	TMMIPs	TMNIPs
Pseudo-first-order equation	$Q_{e,cal}$(mg/g)	88.0712	59.5881
	k_1(/min)	0.0578	0.0300
	R^2	0.8871	0.9844
Pseudo-second-order equation	$Q_{e,cal}$(mg/g)	93.7207	72.3066
	k_2(g/(mg min)	0.0010	0.0004
	R^2	0.9904	0.9744

3.5 Recognition of TMMIPs towards 5-FU

The group selectivity of TMMIPs (or TMNIPs) was studied by measuring the uptake of several compounds containing the similar structure to 5-FU (Fig.10). The

tested compounds are 5-FU, uracil and thymine with the same initial concentrations of 5 mmol/L, and their structures of the three pyrimidine compounds were shown in Fig. 10. The error bars have been shown in Fig.10. Reusable two-factor analysis of variance was also used for data significant test. The maximum P-value is 0.0002, which is far less than 0.5, demonstrating the significant influence of adsorbed molecules and adsorbing materials. The adsorption capacities of TMMIPs for 5-FU, uracil and thymine are 94.86, 80.61 and 84.31 mg/g, respectively, showing the better capture behavior of TMNIPs towards 5-FU. Moreover, the differences between the adsorption capacities of TMMIPs and TMNIPs obtained in Fig. 10 are 32.92, 17.46 and 23.17 mg/g for the three compounds, respectively, indicating the cognition for pyrimidine compounds follows the order 5-FU>thymine>uracil. It is obvious that TMMIPs have the best recognition ability towards 5-FU among all three competing compounds, indicating the specific adsorption for the template molecules. On the other hand, the adsorption capacities of TMNIPs towards the three compounds are almost same, suggesting no specific binding sites formed in TMNIPs.
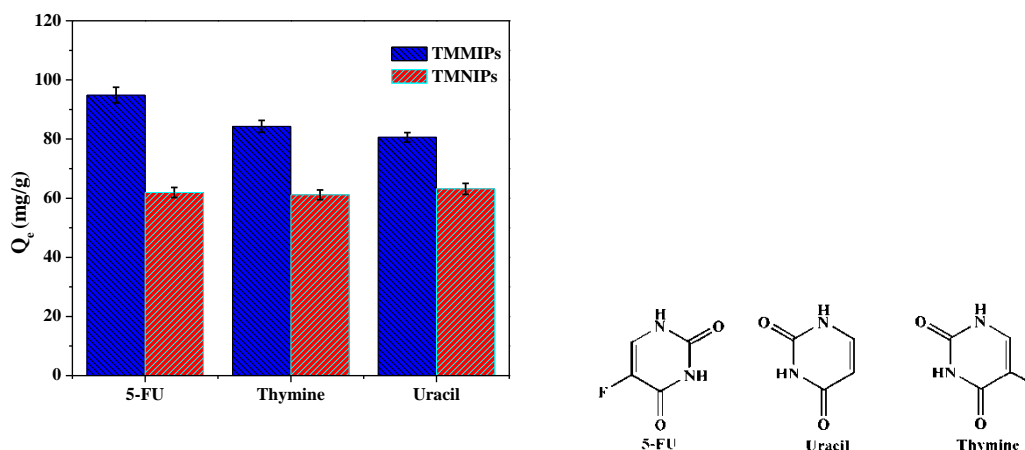

Fig. 10. Adsorption selectivity of TMMIPs and TMNIPs for three pyrimidine compounds in single solute (25℃) and molecule structure of three pyrimidine compounds; error bars indicated standard deviation (N=3).

3.6 Release kinetics of 5-FU

TMMIPs (or TMNIPs) (20 mg) were immersed in 50mL of 5 mmol/L 5-FU solution for 24 h to reach adsorption equilibrium. The loading capacity of TMMIPs and TMNIPs is 94.54 mg/g and 61.77mg/g, respectively. In vitro drug release experiments of the drug-loading TMMIPs (or TMNIPs) were carried out to explore the effects of molecular imprinting and temperature on sustained release.

From Fig. 11 (a), it is obviously seen that the release amount and release rate for TMNIPs are much higher than those of TMMIPs at 25℃ within 100 min. Nearly 70% of 5-FU adsorbed by TMMIPs is released, whereas 84% of 5-FU adsorbed by TMNIPs is released at 25℃. The more specific adsorption in TMMIPs hinders the drug release. As shown in Fig.11 (b), the release amount at higher temperature is higher than that at lower temperature, that is to say, the release rate increases with increasing temperature. When the temperature rises to 45℃, 90.75% of 5-FU is released by TMMIPs, because TMMIPs shrink to become hydrophobic, and the

hydrogen bonding between template and function monomer is disturbed. Moreover, when temperature is below LCST, the 5-FU release was decelerated. It is supposed that the specific sites on the TMMIPs can stabilize the 5-FU binding below the LCST and realize sustained drug release [13, 17, 22].
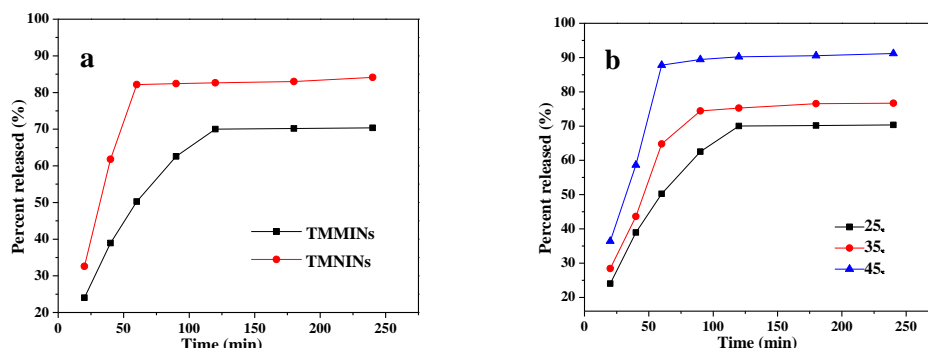
Fig. 11. (a) Release rate of 5-FU from TMMIPs and TMNIPs at 25℃; (b) Release rate of 5-FU from TMMIPs at different temperatures.

3.7 The interaction between NIPAM and 5-FU detected by UV-Vis

The interaction between 5-FU and NIPAM in pre-solution was investigated by UV-Vis analysis, as shown in Fig. 12. There is no obvious shift in the special absorption peak (266 nm) of 5-FU in the absence or presence of NIPAM. While adding NIPAM in pre-solution (the molar ratio of NIPAM/5-FU changes from 0 to 5, keeping 5-FU concentration constant at 0.1 mmol/L), the peak (199 nm) attributed to NIPAM monomer shifts to red and the absorbance intensity of 5-FU continues to increase. This phenomenon could originate from the hydrogen bond interaction between 5-FU and NIPAM, which changes the distribution of electrons around the molecules [47, 48].
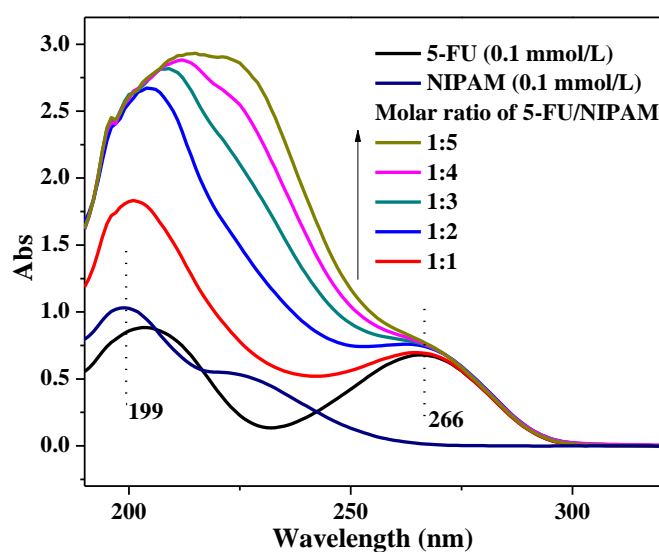
Fig. 12. UV-Vis absorption spectra of 5-FU in the absence or presence of NIPAM in deionized waterwater
(5-FU concentration at 0.01 mmol/L)

15

3.8 Theoretical analysis of TMMIPs affinity towards 5-FU

The optimized geometries of complex PNIPAM/5-FU is presented in Fig. 13 (a). Table 3 shows calculated interaction energies between 5-FU and the functional groups on the surfaces of PNIPAM. To get insight into the 5-FU imprinted site, the binding energy of 5-FU in the imprinted site was calculated according to Eq. (4). ΔE (5-FU/PNIPAM) is equal to -112.24 kJ/mol. It is also verified that 5-FU could be imprinted into the specific site on the surface of TMMIPs.

Table 3. Summary of binding energies of 5-FU/PNIPAM complexes at GGA/PBE (TS method for DFT-D correction)

| Molecular	E (a.u)	ΔE (a.u)	ΔE^{a} (kJ/mol)
5-FU	-513.7434605	-	-
PNIPAM	-6075.1737626	-	-
5-FU/PNIPAM	-6588.9599724	-0.042749	-112.24

[a] 1a.u= 2625.5 kJ/mol

According to Fig.13 (a), 5-FU/PNIPAM complex is constructed to simulate 5-FU binding with imprinted site. Fig. 13 (b) presents the views of the polymer imprinted site towards 5-FU using electrostatic potential (ESP), which shows the distribution of charge on the surface of 5-FU/PNIPAM complex. Negative values are shown as red whereas positive potential values are marked in blue. Correspondingly, the atoms bearing a high negative charge are the good candidates for an interaction with hydrogen donor. The regions beside the imprinted site with strongly positive potential and 5-FU with strongly negative potential are observed. This means that the electrostatic interactions inside the imprinted site with 5-FU are much stronger, and the polar 5-FU can be oriented in specific way. It is also verified that TMMIPs have specific recognition towards 5-FU.
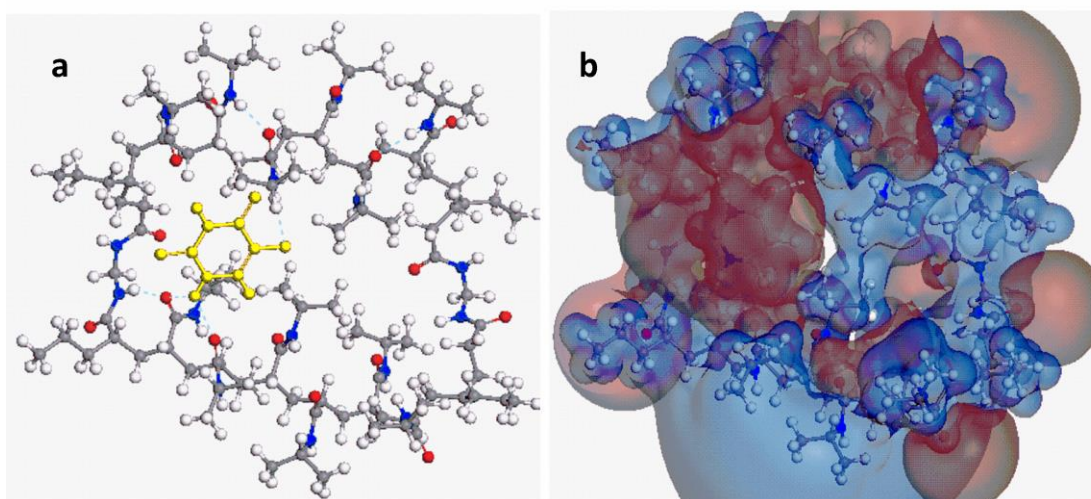
Fig. 13. (a) Optimized structure of PNIPAM/5-FU; (b) ESP isosurface of 5-FU/PNIPAM (positive by blue, negative by red, DMol[3] GGA/PBE)

Atomic charges were calculated by the most used Mulliken population analysis. Mulliken atomic charges in 5-FU and their complexes are quoted in Table 4. For the sake of brevity, only those atoms involved in interactions such as electrostatic interaction and other weak forces responsible for imprinted site are only shown. From Fig. 14 and Table 4, it can be seen that the charge of N1, N3 decreases from -0.386, -0.332 to -0.448, -0.399, separately. The charge of O7 increases from -0.501 to -0.478. These notable changes are due to the formation of hydrogen bonding between 5-FU and the functional group on the surface of PNIPAM. Furthermore, electrostatic interaction can also play exclusive role in imprinting process involving higher binding energy. When template and monomer interact with each other, the initial contact arises from long range electrostatic forces. These electrostatic forces are supplemented by weak forces, such as hydrogen bonding, Van der Waal forces, hydrophobic interactions operating between complementary functional groups located on template and PNIPAM. Consequently upon the template retrieval, specific sites in TMMIPs are thus created, which are accessible for the template rebinding with similar chemical affinity [28, 29, 49, 50].
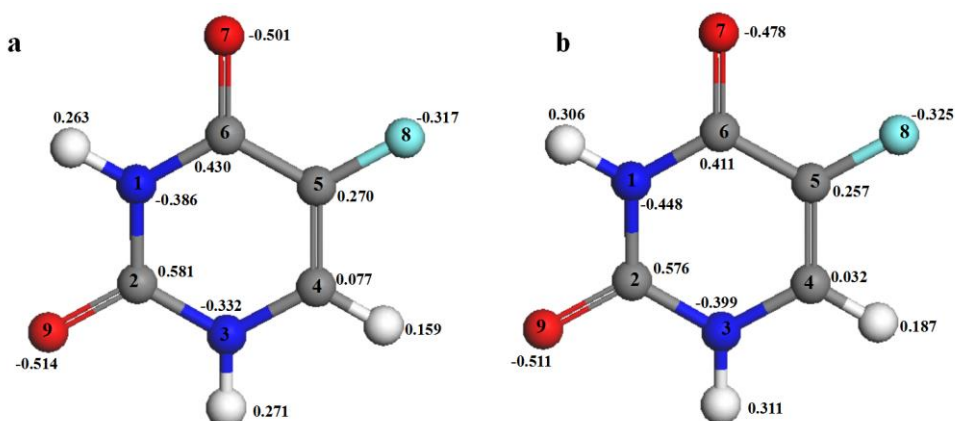
Fig. 14. Atomic charges in 5-FU before (a) and after (b) the formation of complex, calculated by a Mulliken population analysis method.

Table 4. Atomic charges in 5-FU before and after the formation of complex, calculated at GGA/PBE (DNP), in element charges (1.602×10^{-19} C).

Number	Atom	Atomic charge	
		Individual	Complex
1	N	-0.386	-0.448
2	C	0.581	0.576
3	N	-0.332	-0.399
4	C	0.077	0.032
5	C	0.270	0.257
6	C	0.430	0.411
7	O	-0.501	-0.478
8	F	-0.317	-0.325
9	O	-0.514	-0.511

Conclusion

In this study, TMMIPs were prepared and evaluated as adsorbent for recognitive

17

adsorption and controlled release of 5-FU in aqueous solution. The prepared TMMIPs have an average diameter of about 150 nm with a lower critical solution temperature at around 39.2℃, and also display superpara magnetic properties. The adsorption experiment shows that TMMIPs exhibit excellent adsorption capacity (up to 96.53 mg/g at 25℃) and thermo-sensitivity. The adsorption kinetics can be well described by the pseudo-second-order kinetic model, and the isotherm data fit the Langmuir and freundlich models. The selective recognition experiments verified that TMMIPs have affinity and selectivity towards 5-FU. The PNIPAM in TMMIPs exhibits thermo-induced swelling/shrinking transition, and adsorption/release activities could accordingly be modulated by temperature. 5-FU release rate increases with rising temperature, and is 91.17% at 45℃. In addition, DMol^3 program has been used to study the adsorption mechanism in aqueous solution. The interaction binding energy between PNIPAM and 5-FU is -112.24 kJ/mol. The electrostatic potential charges and population analysis confirm the specific imprinted sites are created in TMMIPs, verifying their good adsorption and release behavior. In this work, TMMIPs may achieve three main functions simultaneously, (a) superparamagnetism and targeted at the specific site; (b) selective recognition and adsorption; (c) controlled release applicable in the drug release. With the further clarification of some problems, such as the interference of complicated aqueous environment, biocompatibility and biodegradation, TMMIPs would have enormous potential applications for drug delivery system in the future.

References

[1] E. Fournier, C. Passirani, N. Colin, P. Breton, S. Sagodira, J.-P. Benoit, Development of novel 5-FU-loaded poly(methylidene malonate 2.1.2)-based microspheres for the treatment of brain cancers, Eur J Pharma Biopharm, 57 (2004) 189-197.

[2] D. Cunliffe, A. Kirby, C. Alexander, Molecularly imprinted drug delivery systems, Adv Drug Deliver Rev, 57 (2005) 1836-1853.

[3] T.P. Huynh, P. Pieta, F. D'Souza, W. Kutner, Molecularly imprinted polymer for recognition of 5-fluorouracil by RNA-type nucleobase pairing, Anal Chem, 85 (2013) 8304-8312.

[4] L.Z. Zhu, J.W. Ma, N.Q. Jia, Y. Zhao, H.B. Shen, Chitosan-coated magnetic nanoparticles as carriers of 5-fluorouracil: preparation, characterization and cytotoxicity studies, Colloid Surface B, 68 (2009) 1-6.

[5] A. Kugimiya, T. Mukawa, T. Takeuchi, Synthesis of 5-fluorouracil-imprinted polymers with multiple hydrogen bonding interactions, The Analyst, 126 (2001) 772-774.

[6] F. Puoci, F. Iemma, G. Cirillo, N. Picci, P. Matricardi, F. Alhaique, Molecularly imprinted polymers for 5-fluorouracil release in biological fluids, Molecules, 12 (2007) 805-814.

[7] F. Puoci, F. Iemma, N. Picci, Stimuli-responsive molecularly imprinted polymers for drug delivery: A review, Curr Drug deliv, 5 (2008) 85-96.

[8] W.F. Liu, H.J. Zhao, Y.Z. Yang, X.G. Liu, B.S. Xu, Reactive carbon microspheres prepared by surface-grafting 4-(chloromethyl) phenyl trimethoxy silane for preparing molecularly imprinted polymer, Appl Surf Sci, 277 (2013) 146-154.

[9] H. Wang, J.H. Yi, S. Mukherjee, P. Banerjee, S.Q. Zhou, Magnetic/NIR-thermally responsive hybrid nanogels for optical temperature sensing, tumor cell imaging and triggered drug release, Nanoscale, 6 (2014) 13001-13011.

[10] H.Q. Zhang, Water-compatible molecularly imprinted polymers: Promising synthetic substitutes for biological receptors, Polymer, 55 (2014) 699-714.

[11] Y.Q. Lv, T.W. Tan, F. Svec, Molecular imprinting of proteins in polymers attached to the surface of nanomaterials for selective recognition of biomacromolecules, Biotechnol Adv, 31 (2013) 1172-1186.

[12] D.L. Xiao, P. Dramou, N.Q. Xiong, H. He, H. Li, D.H. Yuan, H. Dai, Development of novel molecularly imprinted magnetic solid-phase extraction materials based on magnetic carbon nanotubes and their application for the determination of gatifloxacin in serum samples coupled with high performance liquid chromatography, J Chromatogr A, 1274 (2013) 44-53.

[13] S.F. Xu, H.Z. Lu, X.W. Zheng, L.X. Chen, Stimuli-responsive molecularly imprinted polymers: versatile functional materials, J Mater Chem C, 1 (2013) 4406-4422.

[14] F. Chen, X.P. Jiang, T.R. Kuang, L.Q. Chang, D.J. Fu, M.Q. Zhong, Polyelectrolyte/mesoporous silica hybrid materials for the high performance multiple-detection of pH value and temperature, Polym Chem, 6 (2015) 3529-3536.

[15] F. Chen, X.P. Jiang, T.R Kuang, L.Q Chang, M.Q. Zhong, Effect of nanoporous structure and polymer brushes on the ionic conductivity of poly(methacrylic acid)/anode aluminum oxide hybrid membranes, RSC Adv, 5 (2015) 70204-70210.

[16] C.J. Zhang, X.P. Jia, Y.Z. Wang, M. Zhang, S. Yang, J.X. Guo, Thermosensitive molecularly imprinted hydrogel cross-linked with N-malely chitosan for the recognition and separation of BSA, J Sep Sci, 37 (2014) 419-426.

[17] R.C. Dong, J.H. Li, H. Xiong, W.H. Lu, H.L. Peng, L.X. Chen, Thermosensitive molecularly imprinted polymers on porous carriers: preparation, characterization and properties as novel adsorbents for bisphenol A, Talanta, 130 (2014) 182-191.

[18] D. Ran, Y.Z. Wang, X.P. Jia, C. Nie, Bovine serum albumin recognition via thermosensitive molecular imprinted macroporous hydrogels prepared at two different temperatures, Anal Chim Acta, 723 (2012) 45-53.

[19] T. Hien Nguyen, R.J. Ansell, N-isopropylacrylamide as a functional monomer for noncovalent molecular imprinting, Journal Mol Recognit, 25 (2012) 1-10.

[20] F.X. Gao, X.L. Zhao, X.W. He, W.Y. Li, Y.K. Zhang, A pH and temperature dual-responsive macroporous molecularly imprinted cryogel for enhanced recognition capability towards ovalbumin, Anal Methods, 5 (2013) 6700-6708.

[21] Y. Ma, Y. Zhang, M. Zhao, X.Z. Guo, H.Q. Zhang, Efficient synthesis of narrowly dispersed molecularly imprinted polymer microspheres with multiple stimuli-responsive template binding properties in aqueous media, Chem

631   Commun, 48 (2012) 6217-6219.

632 [22] J.M. Pan, H. Hang, X.X. Li, W.J. Zhu, M.J. Meng, X.H. Dai, J.D. Dai, Y.S Yan,
633   Fabrication and evaluation of temperature responsive molecularly imprinted
634   sorbents based on surface of yeast via surface-initiated AGET ATRP, Appl Surf
635   Sci, 287 (2013) 211-217.

636 [23] T. Jing, H.R. Du, Q. Dai, H. Xia, J.W. Niu, Q.L. Hao, S.R. Mei, Y.K. Zhou,
637   Magnetic molecularly imprinted nanoparticles for recognition of lysozyme,
638   Biosens Bioelectron, 26 (2010) 301-306.

639 [24] C.H. Hu, J. Deng, Y.B. Zhao, L.S. Xia, K.H. Huang, S.Q. Ju, N. Xiao, A novel
640   core-shell magnetic nano-sorbent with surface molecularly imprinted polymer
641   coating for the selective solid phase extraction of dimetridazole, Food chem, 158
642   (2014) 366-373.

643 [25] L.C. Xu, J.M. Pan, J.D. Dai, X.X. Li, H. Hang, Z.J. Cao, Y.S Yan, Preparation of
644   thermal-responsive magnetic molecularly imprinted polymers for selective
645   removal of antibiotics from aqueous solution, J Hazard Mater, 233-234 (2012)
646   48-56.

647 [26] Q.P. You, Y.P. Zhang, Q.W. Zhang, J.F. Guo, W.H. Huang, S.Y. Shi, X.Q. Chen,
648   High-capacity thermo-responsive magnetic molecularly imprinted polymers for
649   selective extraction of curcuminoids, J Chromatogr A, 1354 (2014) 1-8.

650 [27] R.J. Gui, Y.F. Wang, J. Sun, Encapsulating magnetic and fluorescent mesoporous
651   silica into thermosensitive chitosan microspheres for cell imaging and controlled
652   drug release in vitro, Colloids Surf B Biointerfaces, 113 (2014) 1-9.

653 [28] B.B. Prasad, G. Rai, Study on monomer suitability toward the template in
654   molecularly imprinted polymer: an ab initio approach, Spectrochim Acta. Part A
655   Mol biomol spectrosc, 88 (2012) 82-89.

656 [29] P. Lulinski, M. Sobiech, T. Zolek, D. Maciejewska, A separation of tyramine on a
657   2-(4-methoxyphenyl)ethylamine imprinted polymer: an answer from theoretical
658   and experimental studies, Talanta, 129 (2014) 155-164.

659 [30] R.G. Zhang, L.X. Ling, Z. Li, B.J. Wang, Solvent effects on $Cu_2O(111)$ surface
660   properties and CO adsorption on $Cu_2O(111)$ surface: A DFT study, Appl Catal A-
661   Gen, 400 (2011) 142-147.

662 [31] Z.M. Xing, C.L. Wang, J. Yan, L. Zhang, L. Li, L.S. Zha, Dual stimuli
663   responsive hollow nanogels with IPN structure for temperature controlling drug
664   loading and pH triggering drug release, Soft Matter, 7 (2011) 7992.

665 [32] M. Mananghaya, E. Rodulfo, G.N. Santos, A density functional theory-based
666   investigation of the functionalization density dependence of the solubility of
667   single-walled carbon nanotubes, IJSRET,12 (2012) 2229-5518.

668 [33] L.F. Li, L. Chen, W.F. Liu, Y.Z. Yang, X.G. Liu, Y.Z. Chen, Preparation and
669   characterization of 5-fluorouracil surface-imprinted thermosensitive magnetic
670   microspheres, Monatsh Chem, 146 (2014) 441-447.

671 [34] Z.J. Zuo, W. Huang, P.D. Han, Z.H. Li, Solvent effects for CO and H_2 adsorption
672   on Cu_2O (111) surface: A density functional theory study, Appl Surf Sci, 256
673   (2010) 2357-2362.

674 [35] C. Yu, X.M. Fan, L.M. Yu, T.J. Bandosz, Z.B. Zhao, J.S. Qiu, Adsorptive
675   removal of thiophenic compounds from oils by activated carbon modified with
676   concentrated nitric acid, Energ Fuel, 27 (2013) 1499-1505.

677 [36] M.R. Mauricio, G.M. Carvalho, E. Radovanovic, E.C. Muniz, A.F. Rubira,
678   Analysis of poly(N-isopropylacrylamide) grafted onto the surface of PET films
679   by SI-ATRP technique, Mater Sci Eng C, 29 (2009) 594-598.

680 [37] H. Kempe, A.P. Pujolràs, M. Kempe, Molecularly imprinted polymer

681 nanocarriers for sustained release of erythromycin, Pharm Res, 32 (2015)
682 375-388.

[38] L. Chen, H. Zhang, L.F. Li, Y.Z. Yang, X.G. Liu, B.S. Xu, Thermoresponsive
684 hollow magnetic microspheres with hyperthermia and controlled release
685 properties, J Appl Polym Sci, 132 (2015), DOI:10.1002/app.42617

[39] P.E. Feuser, L.S. Bubniak, M.C.S. Silva, A.C Viegas, Encapsulation of magnetic
687 nanoparticles in poly(methyl methacrylate) by miniemulsion and evaluation of
688 hyperthermia in U87MG cells, Eur Polym J, 380 (2015)355-365

[40] M. Mazzotti, Equilibrium theory based design of simulated moving bed
690 processes for a generalized Langmuir isotherm, J Chromatogr A, 1126 (2006)
691 311-322.

[41] S.J. Allen, G. McKay, J.F. Porter, Adsorption isotherm models for basic dye
693 adsorption by peat in single and binary component systems, J Colloid Interf Sci,
694 280 (2004) 322-333.

[42] F.F. Duan, C.Q Chen, G.Z. Wang, Y.Z. Yang, X.G. Liu, Y. Qin, Efficient
696 adsorptive removal of dibenzothiophene by graphene oxide-based surface
697 molecularly imprinted polymer, RSC Adv, 4 (2014) 1469-1475.

[43] J.X. Wang, J.M. Pan, Y.J. Yin, R.R. Wu, X.H. Dai, J.D. Dai, L. Gao, H.X. Ou,
699 Thermo-responsive and magnetic molecularly imprinted Fe_3O_4@carbon
700 nanospheres for selective adsorption and controlled release of
701 2,4,5-trichlorophenol, J Ind Eng Chem, 25 (2015) 321-328.

[44] Y. Ho, G. McKay, The sorption of lead (II) ions on peat, Water Res, 33 (1999)
703 578-584.

[45] Y.S. Ho, G. McKay, Pseudo-second order model for sorption processes, Process
705 Biochem, 34 (1999) 451-465.

[46] F.F. Duan, C.Q. Chen, L. Chen, Y.J. Sun, Y.W. Wang, Y.Z. Yang, X.G Liu, Y. Qin,
707 Preparation and Evaluation of Water-Compatible Surface Molecularly Imprinted
708 Polymers for Selective Adsorption of Bisphenol A from Aqueous Solution, Ind
709 Eng Chem Res, 53 (2014) 14291-14300.

[47] X.F. Lu, Y.f. Shi, H.L. Lv, Y.Y. Fu, D. Ma, W. Xue, Preparation and
711 characterization of molecularly imprinted poly (hydroxyethyl methacrylate)
712 microspheres for sustained release of gatifloxacin, J Mater Sci-Mater M, 25
713 (2014) 1461-1469.

[48] Y.F. Shi, H.L Lv, X.F. Lu, Y.X. Huang, Y. Zhang, W. Xue, Uniform molecularly
715 imprinted poly (methacrylic acid) nanospheres prepared by precipitation
716 polymerization: the control of particle features suitable for sustained release of
717 gatifloxacin, J Mater Chem, 22 (2012) 3889-3898.

[49] T. Koubský, L. Kalvoda, Application of ab-initio molecular electronic structure
719 calculations of radiolytic and hydrolytic stabilities of prospective extractants, J
720 Radioanal Nucl Ch, 304 (2014) 227-235.

[50] R. Kar, S. Pal, Effect of solvents having different dielectric constants on
722 reactivity: A conceptual DFT approach, Int J Quantum Chem, 110 (2010)
723 1642-1647.